

Spatially-Resolved Photoluminescence Study of Temperature Dependence of Exciton Inelastic Scattering Processes in a ZnO Thin Film

メタデータ	言語: English 出版者: The Physical Society of Japan 公開日: 2020-08-03 キーワード (Ja): キーワード (En): 作成者: 中山, 正昭, 中山, 陽次郎 メールアドレス: 所属: Osaka City University, Osaka City University
URL	https://ocu-omu.repo.nii.ac.jp/records/2020042

Spatially-Resolved Photoluminescence Study of Temperature Dependence of Exciton Inelastic Scattering Processes in a ZnO Thin Film

Masaaki Nakayama, Yojiro Nakayama

Citation	Journal of the Physical Society of Japan, 88(8); 083706
Issue Date	2019-07-25
Type	Journal Article
Textversion	Author
Rights & Relation	©2019 The Physical Society of Japan. The following article has been accepted by Journal of the Physical Society of Japan. This is the accepted manuscript version. After it is published, it will be found at https://doi.org/10.7566/JPSJ.88.083706 .
DOI	10.7566/JPSJ.88.083706

Self-Archiving by Author(s)
Placed on: Osaka City University

Spatially-Resolved Photoluminescence Study of Temperature Dependence of Exciton
Inelastic Scattering Processes in a ZnO Thin Film

Masaaki Nakayama and Yojiro Nakayama

*Department of Applied Physics and Electronics, Graduate School of Engineering, Osaka City
University, Sugimoto, Sumiyoshi-ku, Osaka 558-8585, Japan*

We have investigated the temperature dependence of exciton inelastic scattering processes, exciton-exciton scattering and exciton-electron scattering, in a ZnO thin film using spatially-resolved photoluminescence (PL) spectroscopy. It was found that the PL band due to the exciton inelastic scattering process is selectively observed at a spot around a film edge away from an excitation spot. The selective observation enabled us to measure precisely the PL-peak energy. The quantitative analysis of the temperature dependence of the PL-peak energy reveals that the exciton-exciton scattering, which occurs in a temperature region from 10 to ~160 K, changes to the exciton-electron scattering in a higher temperature region up to room temperature.

From the 1960s, ZnO has attracted much attention in physics and applications related to the excitonic properties mainly because the exciton binding energy, $E_b=60$ meV, is sufficiently larger than the thermal energy at room temperature (RT).¹⁾ Prominent phenomena in the excitonic properties are exciton inelastic scattering processes such as exciton-exciton scattering and exciton-electron scattering, which produce an optical gain leading to stimulated emission.²⁾ In the exciton-exciton scattering process under energy and momentum conservation, one exciton with a hydrogenic quantum number $n=1$ is scattered into an $n \geq 2$ state including $n=\infty$ (the continuum state), while the other is scattered onto the photon-like region in the lower polariton (LP) branch. Subsequently, the photon-like LP is converted to the so-called P emission.³⁾ The P emission has been mainly observed in the following wide band-gap semiconductors in a low temperature region: ZnO,^{3,4)} CdS,^{5,6)} GaN,⁷⁻⁹⁾ $\text{In}_x\text{Ga}_{1-x}\text{N}$,¹⁰⁾ and CuI.^{11,12)} In the exciton-electron scattering process under energy and momentum conservation, an electron around a conduction-band bottom is scattered to a hot electron. On the other hand, an exciton with $n=1$ is scattered onto the photon-like LP leading to photon conversion,³⁾ the so-called H emission.¹³⁾ The electron contributing to exciton-electron scattering in undoped semiconductors is provided by thermal dissociation of excitons; therefore, the H emission is usually observed in a relatively high temperature region in wide band-gap semiconductors such as ZnO,⁴⁾ CdS,⁵⁾ GaN,^{9,14)} and cuprous halides (CuCl, CuBr, and CuI).¹³⁾

The excitonic system in ZnO is highly stable because of $E_b=60$ meV. Thanks to that, excitonic lasing and/or stimulated emission at RT in ZnO were intensively investigated.¹⁵⁻¹⁹⁾ In these works, the mechanism for excitonic lasing and/or stimulated emission was assigned to the exciton-exciton scattering process. In contrast, it was recently reported that the exciton-electron scattering occurs in a ZnO film, which was composed of tightly-packed microcrystals prepared by a thermochemical deposition method, in the temperature region from ~ 150 K to RT.⁴⁾ Thus, the exciton inelastic scattering process in ZnO at RT is still controversial.

In the present work, we have investigated the exciton inelastic scattering process as a function of temperature from 10 to 290 K (RT) in a ZnO thin film prepared by a pulsed laser deposition (PLD) method using spatially-resolved photoluminescence (PL) spectroscopy. We

found that the PL band due to the exciton inelastic scattering process is selectively observable at a spot along a film edge which is spatially separated from an excitation spot. This is a key phenomenon in this work. We systematically measured the spatially-resolved PL spectrum at the spatially-separated spot as a function of temperature at various excitation powers. We quantitatively discuss the temperature dependence of the PL-peak energy from the viewpoint of the transition from the exciton-exciton scattering to the exciton-electron scattering.

The sample was a crystalline ZnO thin film with a thickness of 1.0 μm grown on a (0001) Al_2O_3 substrate at 650 $^\circ\text{C}$ with a PLD method. The laser for deposition was the fourth harmonic generation light (266 nm) of a pulsed yttrium-aluminum-garnet (YAG) laser with a fluence of $\sim 2.5 \text{ J/cm}^2$, a pulse width of 5 ns, and a repetition rate of 10 Hz. A commercially supplied plate of ZnO with a purity of 99.99% was used as a target. The partial pressure of O_2 during the deposition process was kept at 1.3 Pa. The film thickness was calibrated with a profilometer. It was confirmed from X-ray diffraction patterns that the growth direction of the ZnO thin film is just along the c axis.

The excitation light in PL measurements was the third harmonic generation light (355 nm) of a pulsed YAG laser with a pulse width of 1.0 ns and a repetition rate of 10 kHz. Figure 1 shows the schematic diagram of the measurement system of spatially-resolved PL spectroscopy. For excitation and collection of PL, an objective lens with a numerical aperture of 0.13 and a focal length of 40 mm was used. We observed a spatial PL image using a CMOS profiler, removing a pinhole with a diameter of 50 μm from the light path. The magnification of the measurement system was 4.5 times, which was calibrated using a micro-ruler. In measuring a spatially-resolved PL spectrum, we selected the PL image using the pinhole, the position of which was monitored with the CMOS profiler: The spatial resolution was 11 μm . To measure PL spectra, a cooled charge coupled device attached to a 32-cm single monochromator with a spectral resolution of 0.15 nm was used. The sample temperature was controlled with a low-vibration-type closed cycle helium cryostat: The vibration amplitude was $\sim 2 \mu\text{m}$.

Figure 2 shows the spatial PL image of the ZnO thin film at the excitation fluence of 0.10 mJ/cm^2 at 10 K, where the normalized PL intensity is indicated by the color scale and the white dashed line depicts the film edge. It is obvious that a PL spot appears around the film

edge which is spatially separated from an excitation spot. Note that spatial PL images similar to Fig. 2 were observed in the whole temperature region up to 290 K. Figure 3 shows the spatially-resolved PL spectra at various excitation fluences at (a) the excitation spot and (b) the spatially-separated spot at 10 K, where the PL intensity is normalized by the maximum intensity at each excitation fluence and E_A , E_b , and $E_{b,M}$ indicate the A-exciton energy, exciton binding energy, and biexciton binding energy, respectively. From the free exciton PL band under a weak excitation condition with a He-Cd laser, E_A was obtained to be 3.3750 ± 0.0002 eV, which is in agreement with E_A in a bulk crystal,¹⁾ and $E_{b,M}=14.7$ meV was taken from Ref. 20. In Fig. 3(a), a PL band labeled M, the peak energy of which almost agrees with $E_A - E_{b,M}$, is observed. The M-PL band exhibits a low energy tail peculiar to the biexciton PL, the so-called inverse Boltzmann line shape. Thus, the M-PL band is attributed to the biexciton. At $0.35I_0$, a PL band labeled P, the peak energy of which is almost equal to $E_A - E_b$, appears with a threshold-like nature and it becomes dominant accompanied by a low energy shift with an increase in excitation fluence. These characteristics reflect the exciton-exciton scattering process. The PL-peak energy of the P emission, E_P , is given by³⁾

$$E_P = E_{A,n=1} - (E_{A,n \geq 2} - E_{A,n=1}) - 3\sigma k_B T_{\text{eff}}, \quad (1)$$

where $E_{A,n}$ is the A-exciton energy with n , $E_{A,n=1}=E_A$, T_{eff} is an effective temperature, and σ is a positive constant smaller than unity. In this case, the exciton-exciton scattering into the $n=\infty$ state occurs. The low energy shift of the P-PL peak energy results from an increase in T_{eff} . The threshold-like appearance of the P-PL band in Fig. 3(a) reflects the occurrence of stimulated emission with an optical gain.^{10,11)}

At the spatially-separated spot, as shown in Fig. 3(b), the PL spectral profile dramatically changes from that at the excitation spot shown in Fig. 3(a). The M-PL band is remarkably suppressed by the reabsorption effect on the PL light traveling from the excitation spot to the film edge. On the other hand, the reabsorption effect on the P-PL band is not considerable. Note that the low energy tail of the M-PL band overlaps with the P-PL band; however, the P-PL band is highlighted at the spatially-separated spot. This fact suggests that the photon-like LP, which is the final state of the exciton inelastic scattering process as described above, propagates along the in-plane direction from the excitation spot, and then it

is converted to a photon corresponding to the P emission at the film edge at which the translational symmetry is broken.²¹⁾ As a result, the P-PL band is selectively observed at the spatially-separated spot. The selective observation of the PL band from the P emission or H emission at the spatially-separated spot was confirmed in the whole temperature region up to 290 K. Note that a tail of the exciton absorption band extends to a low energy side with an increase in temperature owing to the Urbach rule; however, the polariton nature of the P emission and H emission prevents the reabsorption effect on the P-PL and H-PL bands. Thus, we could precisely observe the PL band due to the exciton-exciton scattering or exciton-electron scattering using spatially-resolved PL spectroscopy. This is a prominent merit in this work.

In a relatively high temperature region, it is expected that the H emission due to exciton-electron scattering occurs.^{4,9,13,14)} The PL-peak energy of the H emission, E_H , is given by³⁾

$$E_H = E_A - \frac{3}{2} \left(\frac{M_X}{m_e} - 1 + 2\delta \sqrt{\frac{M_X}{m_e}} \right) k_B T_{\text{eff}}, \quad (2)$$

where M_X and m_e are the effective masses of the exciton and electron, respectively, and δ is a positive constant smaller than unity. For ZnO, m_e is $0.28m_0$,²²⁾ where m_0 is the free electron mass, and $M_X = m_e + m_h$ is $0.87m_0$, where m_h is the hole effective mass in the A valence band: $0.59m_0$.²²⁾ The unique feature of the H emission is that $E_H - E_A$ is proportional to temperature and becomes zero at absolute zero temperature.

Figure 4(a) shows the PL spectra observed at the spatially-separated spot at temperatures from 10 to 290 K with a step of 10 K, where E_A at each temperature is the origin of photon energy, E_{ph} , and the PL spectrum is normalized by the maximum intensity at each temperature. We selected the PL spectrum with the lowest peak energy corresponding to the lowest T_{eff} at each temperature. The temperature dependence of E_A was calculated using the following Varshni formula: $E_A(T) = E_A(0) - \alpha T^2 / (T + \beta)$, where $\alpha = 0.65$ meV/K and $\beta = 660$ K for ZnO.²³⁾ The value of $E_A(0)$ was estimated from experimentally obtained $E_A(10) = 3.3750$ eV using the Varshni formula: 3.3751 eV. We quantitatively analyze the temperature dependence of the spacing between the PL-peak energy, E_{peak} , and E_A , $E_{\text{peak}} - E_A$, as shown in Fig. 4(b), where the solid and dashed lines indicate the fitted results using Eqs. (1) and (2), respectively.

In the fitting process, we assumed that T_{eff} is equal to the lattice temperature. In the temperature region from 10 to 160 K, the solid line well explain the temperature dependence of $E_{\text{peak}}-E_{\text{A}}$, where the fitting parameter in Eq. (1) is $\sigma=0.46$. At absolute zero temperature, the solid line reaches $E_{\text{peak}}-E_{\text{A}}=0.060$ eV corresponding to the exciton binding energy, which demonstrates the appropriateness of the fitted result. Thus, the exciton-exciton scattering occurs in the temperature region from 10 to 160 K. In contrast, in the temperature region from 200 to 290 K, the dashed line fits the temperature dependence of $E_{\text{peak}}-E_{\text{A}}$, where the fitting parameter in Eq. (2) is $\delta=0.42$. The dashed line reaches $E_{\text{peak}}-E_{\text{A}}=0$ eV at absolute zero temperature, which is an inevitable result from Eq. (2). Thus, it is concluded that the exciton-electron scattering occurs in the temperature region from 200 to 290 K. At the temperatures of 170, 180, and 190 K, the value of $E_{\text{peak}}-E_{\text{A}}$ slightly deviates from the dashed line. This deviation may result from a slight change of δ : The δ value is estimated to be ~ 0.44 . Since the values of σ in Eq. (1) and δ in Eq. (2) are phenomenological in this work, the quantitative discussion is beyond the scope of this paper. If we assume the occurrence of exciton-hole scattering, δ is estimated to be 1.3 using Eq. (2), where m_{e} is replaced by m_{h} . The value of δ should be smaller than unity; therefore, we can exclude the exciton-hole scattering. We did not observe the coexistence of the P-PL and H-PL bands in the whole temperature region. In Ref. 4, in which the temperature induced transition from the exciton-exciton scattering process to the exciton-electron scattering process was also investigated in a ZnO film, the coexistence of the two PL bands was not observed. Therefore, the experimental fact phenomenologically suggests that the two scattering processes cannot coexist. This may be due to that the occurrence of the exciton-electron scattering process, which results from thermal dissociation of excitons in the high temperature region, prevents that of the exciton-exciton scattering process. There is no available theory to discuss whether the two scattering processes coexist or not.

In summary, we have investigated the transition of the exciton inelastic scattering process from exciton-exciton scattering to exciton-electron scattering in a ZnO thin film with an increase in temperature from 10 to 290 K (RT) using spatially-resolved PL spectroscopy. We selectively observed the PL band due to the exciton inelastic scattering process at a spot around a film edge which is spatially separated from an excitation spot. This phenomenon

originates from the spatial propagation of the photon-like LP corresponding to the final state of the exciton inelastic scattering process. The selective observation of the P-PL and H-PL bands enabled us to detect precisely the peak energies. We quantitatively analyzed the temperature dependence of the PL-peak energy. As a result, we clearly showed that the exciton-exciton scattering, which occurs in the temperature region from 10 to 160 K, changes to the exciton-electron scattering in the higher temperature region up to 290 K.

Acknowledgement This work was supported by JSPS KAKENHI Grant Number 18K03494.

References

- 1) C. Klingshirn, J. Fallert, H. Zhou, J. Sartor, C. Thiele, F. Maier-Flaig, D. Schneider, and H. Kalt, *Phys. Status Solidi B* **247**, 1424 (2010).
- 2) S. W. Koch, H. Haug, G. Schmieder, W. Bohnert, and C. Klingshirn, *Phys. Status Solidi B* **89**, 431 (1978).
- 3) C. Klingshirn, *Phys. Status Solidi B* **71**, 547 (1975).
- 4) R. Matsuzaki, H. Soma, K. Fukuoka, K. Kodama, A. Asahara, T. Suemoto, Y. Adachi, and T. Uchino, *Phys. Rev. B* **96**, 125306 (2017).
- 5) T. Fischer and J. Bille, *J. Appl. Phys.* **45**, 3937 (1974).
- 6) K. Bohnert, G. Schmieder, and C. Klingshirn, *Phys. Status Solidi B* **98**, 175 (1980).
- 7) J. Holst, L. Eckey, A. Hoffmann, I. Broser, B. Schöttker, D. J. As, D. Schikora, and K. Lischka, *Appl. Phys. Lett.* **72**, 1439 (1998).
- 8) S. Kurai, A. Kawabe, T. Sugita, S. Kubo, Y. Yamada, T. Taguchi, and S. Sakai, *Jpn. J. Appl. Phys.* **38**, L102 (1999).
- 9) H. Tanaka, M. Ando, T. Uemura, and M. Nakayama, *Phys. Status Solidi C* **3**, 3512 (2006).
- 10) M. Nakayama, R. Kitano, M. Ando, and T. Uemura, *Appl. Phys. Lett.* **87**, 092106 (2005).
- 11) I. Tanaka and M. Nakayama, *J. Appl. Phys.* **92**, 3511 (2002).
- 12) H. Ichida, Y. Kanematsu, T. Shimomura, K. Mizoguchi, D. Kim, and M. Nakayama, *Phys. Rev. B* **72**, 045210 (2005).
- 13) C. I. Yu, T. Goto, and M. Ueta, *J. Phys. Soc. Jpn.* **34**, 693 (1973).
- 14) M. Nakayama, H. Tanaka, M. Ando, and T. Uemura, *Appl. Phys. Lett.* **89**, 031909 (2006).
- 15) D. M. Bagnall, Y. F. Chen, Z. Zhu, T. Yao, S. Koyama, M. Y. Shen, and T. Goto, *Appl. Phys. Lett.* **70**, 2230 (1997).
- 16) Z. K. Tang, G. K. L. Wong, P. Yu, M. Kawasaki, A. Ohtomo, H. Koinuma, and Y. Segawa, *Appl. Phys. Lett.* **72**, 3270 (1998).
- 17) Ü. Özgür, A. Teke, C. Liu, S.-J. Cho, H. Morkoç, and H. O. Everitt, *Appl. Phys. Lett.* **84**, 3223 (2004).
- 18) W. M. Kwok, A. B. Djurišić, Y. H. Leung, W. K. Chan, and D. L. Phillips, *Appl. Phys. Lett.* **87**, 093108 (2005).
- 19) A.-S. Gadallah, K. Nomenyo, C. Couteau, D. J. Rogers, and G. Léron del, *Appl. Phys. Lett.*

102, 171105 (2013).

20) J. M. Hvam, G. Blattner, R. Reuscher, and C. Klingshirn, *Phys. Status Solidi B* **118**, 179 (1983).

21) Y. Furukawa and M. Nakayama, *J. Phys. Soc. Jpn.* **87**, 094718 (2018).

22) K. Hümmer, *Phys. Status Solidi B* **56**, 249 (1973).

23) S. Ozaki, T. Mishima, and S. Adachi, *Jpn. J. Appl. Phys.* **42**, 5465 (2003).

Figure captions

Fig.1. (Color online) Schematic diagram of the measurement system of spatially-resolved PL spectroscopy.

Fig. 2. (Color online) Spatial PL image of the ZnO thin film at the excitation fluence of 0.10 mJ/cm² at 10 K, where the normalized PL intensity is indicated by the color scale and the white dashed line depicts the film edge.

Fig. 3. (Color online) Spatially-resolved PL spectra at various excitation fluences at (a) the excitation spot and (b) the spatially-separated spot at 10 K, where the PL intensity is normalized by the maximum intensity at each excitation fluence and E_A , E_b , and $E_{b,M}$ indicate the A-exciton energy, exciton binding energy, and biexciton binding energy, respectively.

Fig.4. (Color online) (a) PL spectra observed at the spatially-separated spot at temperatures from 10 to 290 K with a step of 10 K, where E_A at each temperature is the origin of photon energy, E_{ph} , and the PL spectrum is normalized by the maximum intensity at each temperature. (b) Spacing between the PL-peak energy, E_{peak} , and E_A , $E_{peak}-E_A$, as a function of temperature, where the solid and dashed lines indicate the fitted results using Eqs. (1) and (2), respectively.

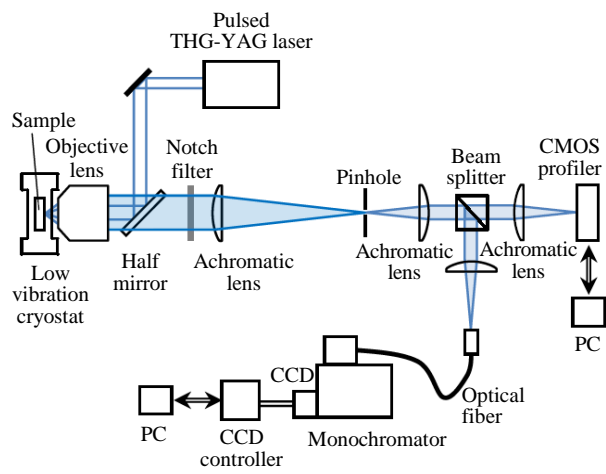


Fig. 1

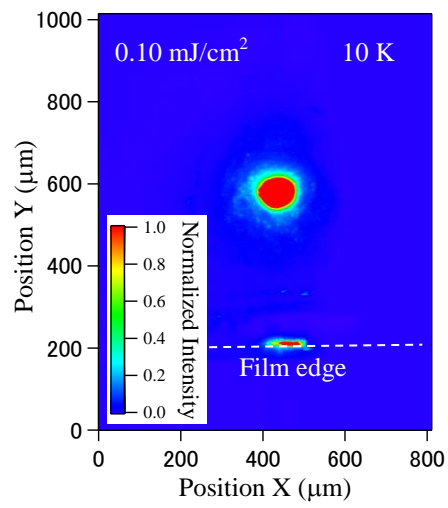


Fig. 2

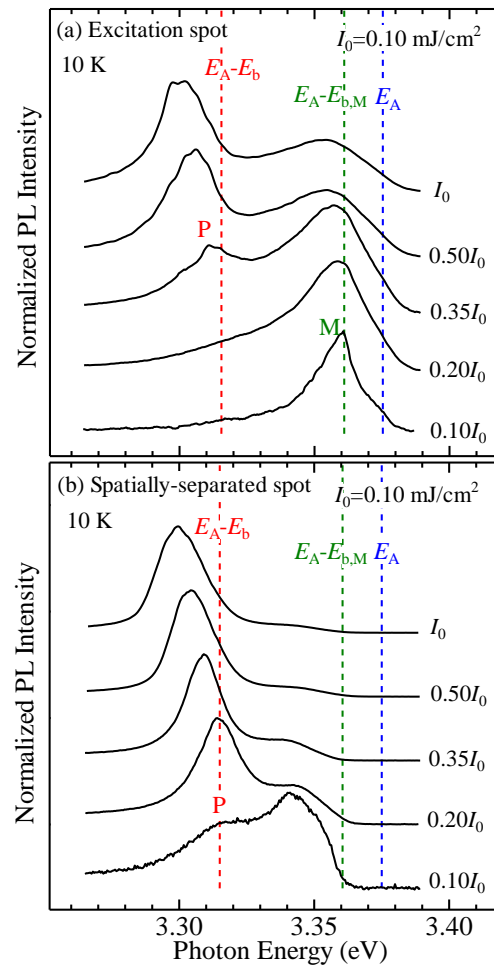


Fig. 3

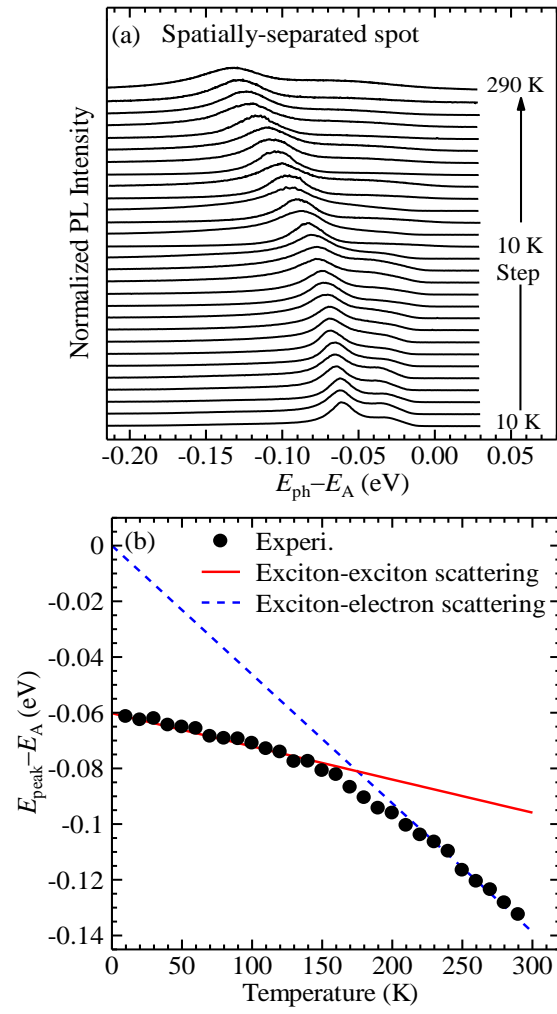


Fig. 4